SMOS L1 Product Performance Status Report

Code : SO-TN-DME-L1PP-0246
Issue : 1.0
Date : 05/11/10

	Name	Function	Signature
Prepared by	A. Gutiérrez	Project Engineer	
Checked by	J. Barbosa	Quality A. Manager	
Approved by	J. Barbosa	Project Manager	

DEIMOS Engenharia
Av. D. João II, Lote 1.17, Torre Zen, 10º,
1998-023 Lisboa, PORTUGAL
Tel: +351 21 893 3013
Fax: +351 21 896 9099
E-mail: mailto:deimos@deimos.com.pt

This page intentionally left blank

Document Information

Contract Data	Classification
Contract Number: 4000101241/10/I-AM	**Internal** ☐ **Public** ☐
Contract Issuer: ESA	**Industry** ☐ **Confidential** ☑

Internal Distribution		
Name	Unit	Copies

External Distribution		
Name	Organisation	Copies
Jean-Claude Debruyn	ESA	1
Steven Delwart	ESA	1

Archiving	
Word Processor:	MS Word 2000
File Name:	SO-TN-DME-L1PP-0246-Product-Performance-Status-Report-E1-R0
Archive Code:	SO-TN-DME-L1PP-0246

Document Status Log

Issue	Change description	Date	Approved
1.0	First Delivery to ESA for L1PP v3.5	2010-11-05	

Table of Contents

List of Figures

List of Tables

1. INTRODUCTION

1.1. Purpose and Scope

This document contains the SMOS L1 Product Performance Status Report, in conformance with the tests and expected verification results from the Product Performance Evaluation Plan.

1.2. Acronyms and Abbreviations

BT	Brightness Temperature
FFT	Fast Fourier Transform
FOV	Field of View
FWF	Fringe Washing Function
MIRAS	Microwave Imaging Radiometer by Aperture Synthesis
NIR	Noise Injection Radiometer
PMS	Power Measurement System
TBH	Temperature Brightness at Horizontal polarisation
TBV	Temperature Brightness at Vertical polarisation
TEC	Total Electron Content

1.3. Applicable and Reference Documents

1.3.1. Applicable Documents

Ref.	Code	Title	Issue
AD.1	SO-SOW-ESA-GS-6647	SMOS Expert Support Laboratories for the period 2010-2014-ESL Level 1 Calibration and Reconstruction Statement of Work	1.2
AD.2	SO-RS-ESA-PLM-0003	SMOS System Requirements Document	3.0
AD.3	SO-TN-UPC-PLM-0019	SMOS In Orbit Calibration Plan Phase C-D	1.5
AD.4	ECSS-E-40B	ECSS E-40 Software Engineering Standards	

Table 1: Applicable Documents

1.3.2. Reference Documents

Ref.	Code/Author	Title	Issue
RD.1	EE-MA-DMS-GS-0001-1-5_090313	Earth Explorer Mission CFI Software MISSION CONVENTIONS DOCUMENT	*1.5*
RD.2	PE-TN-ESA-GS-0001	Earth Explorer Ground Segment File Format Standard	*1.3*
RD.3	EE-MA-DMS-GS-0002-3-7-2_080731	Earth Explorer Mission CFI Software GENERAL SOFTWARE USER MANUAL	*2.0*
RD.4	TN from Juha Kainulainen 11-10-2010	On the NIR Drift	*4.2*
RD.5	SO-TN-DME-L1PP-0240	LO Unlock Algorithms in L1PP	*1.0*

Table 2: Reference Documents

2. L1PP V3.5.0 BASELINE

This chapter shows all the algorithm improvements incorporated into L1PP v3.5 and compares the actual improvements to the expected theoretical improvements that should have been achieved in L1 products after the required modifications are performed.

2.1. NIR Averaging Consolidation

2.1.1. Results Analysis

Visual inspection of ANIR1A files from L1PP v3.5 and L1PP v3.4 shows that the consolidation of the new averaged datasets is performed correctly. The contents of the new datasets are identical to the averaged DSR that was included as a last element in the original datasets for L1PP v3.4.

2.2. NIR Antenna Model

2.2.1. Results Analysis

A dedicated reprocessing campaign for all NIR calibration sequences was performed using L1PP v3.5. The objective was to plot all the possible NIR internal calibration temperatures (T_{NA}) for all NIR units and polarisations and analyse the "flatness" of the distribution against the original results from L1PP v3.4

In the following figure, the distribution of calibrated NIR T_{NA} is seen against time, and the seasonal drift observed in [RD.4] is gone.

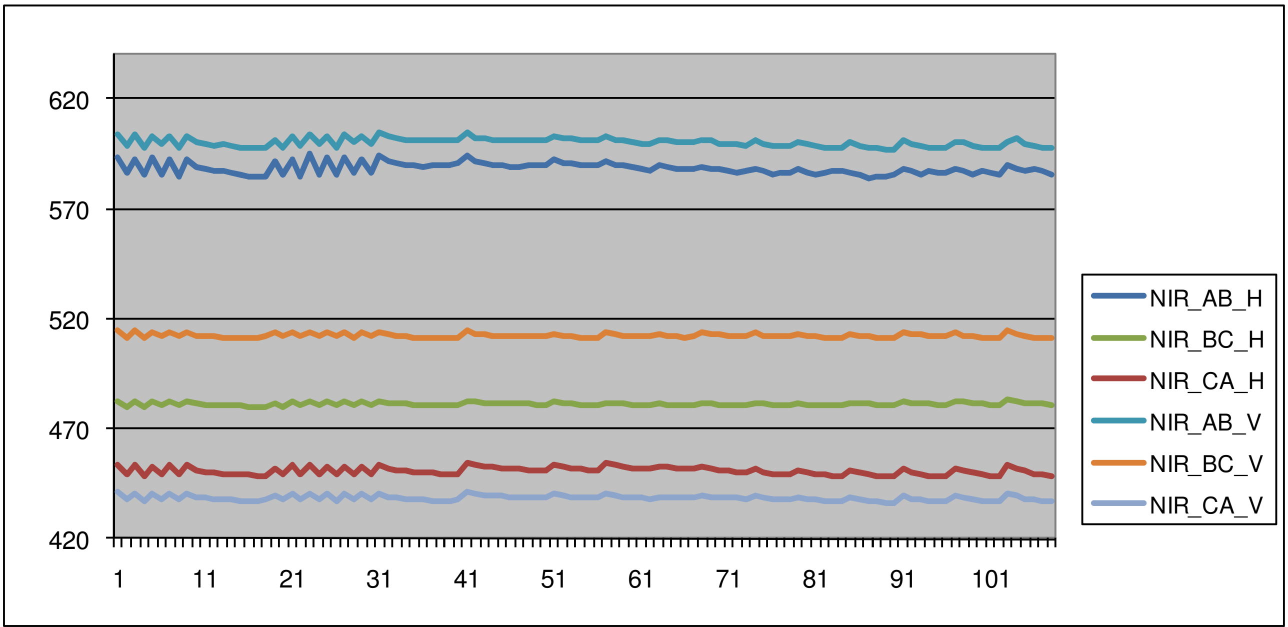

Figure 1: Corrected NIR drift during 2010 in L1PP v3.5

Nevertheless, a small short term ripple is still observed as a consequence of one implementation limitation needed on L1PP v3.5.

In [RD.4], the proposed updated antenna model takes into account a variation of these antenna patch losses with temperature in the following way:

$$L_1 = L_{1,0} + dL_1 + \alpha \cdot \left(\overline{T}_{p7} - T_{p7,0}\right) + \beta \cdot \left(T_{p7} - T_{p7,0}\right) \qquad \textbf{Eq. 1}$$

Where L_{10} is the original value characterized on ground, dL1 an correction term of the on-ground characterized attenuation, $\overline{T}_{p7}$ is the average temperature of the antenna patch during the 6 NIR calibration sequences executed in the last external manoeuvre, T_{p7} is the instantaneous antenna patch temperature and T_{p70} is a reference temperature set to the average temperature of the calibration acquired on the 2nd February for which the rest of coefficients have been obtained.

In SMOS L1 processing of NIR calibration sequences, $\overline{T}_{p7}$ and T_{p7} are necessary identical, as each NIR calibration sequence is processed independently of the others.

2.3. LO Unlock Mitigation

2.3.1. Results Analysis

The following figures represent the FWF Phase interpolation changes between L1PP v3.4 and L1PP v3.5 in face of a LO unlock event:

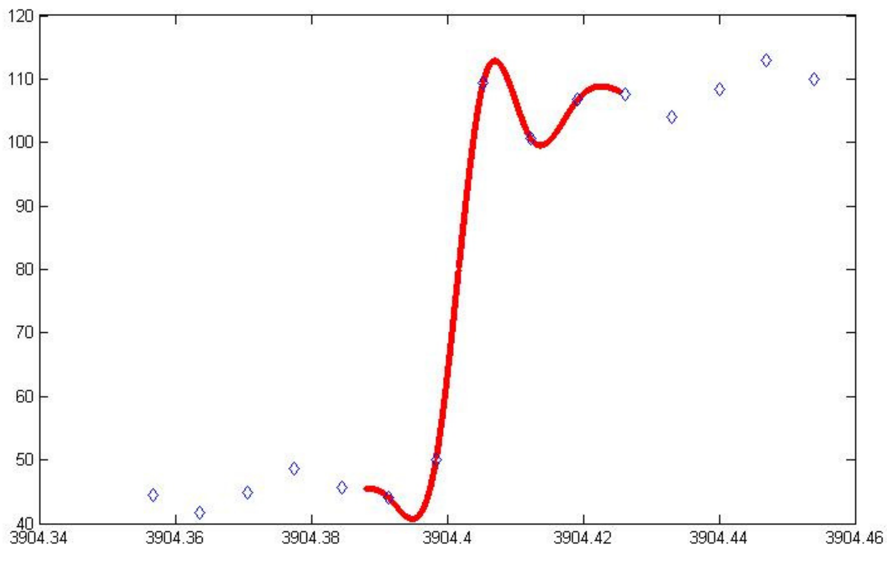

Figure 2: FWF Phase interpolation spline affected by an unlock in L1PP v3.4

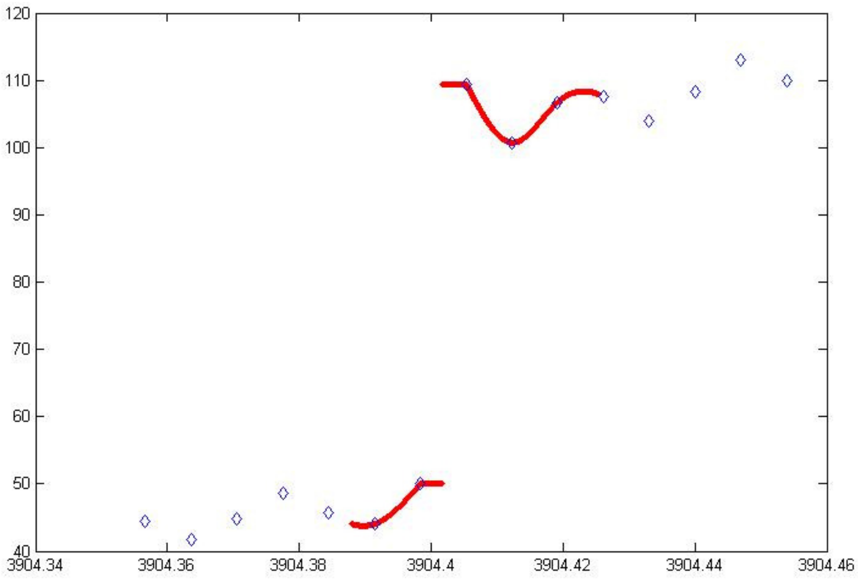

Figure 3: FWF Phase interpolation spline affected by an unlock in L1PP v3.5

The difference in phase between figure 1 and figure 2 is shown in the next one, where the highest difference occurs at the time of the LO unlock event.

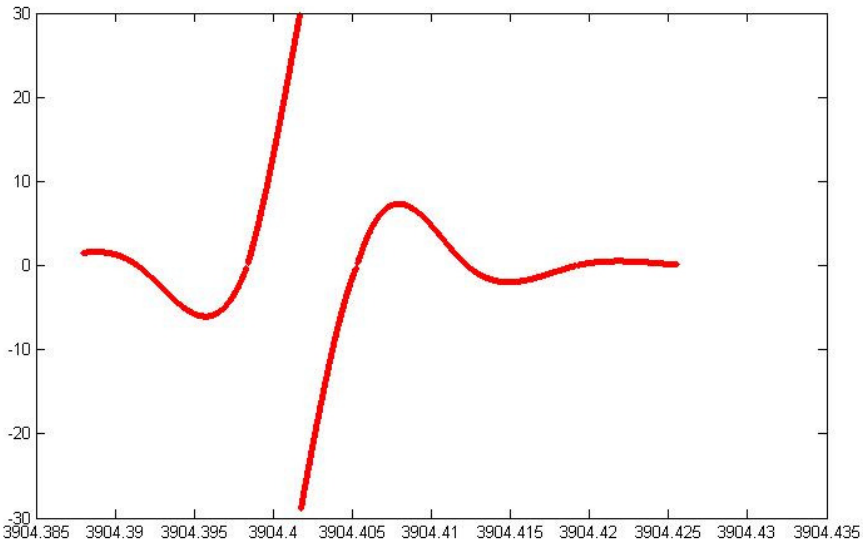

Figure 4: FWF phase interpolation difference between L1PP v3.4 and L1PP v3.5

The baseline analysed in the plots above is AB_03-A_08, although all baselines affected by the unlock event on CMN H1 present a similar behaviour.

On the other hand, unaffected baselines still have the same un-split behaviour in both L1PP v3.4 and L1PP v3.5. As an example, the baseline AB_03-A_01 (not affected by an unlock on H1) is shown in the following figure:

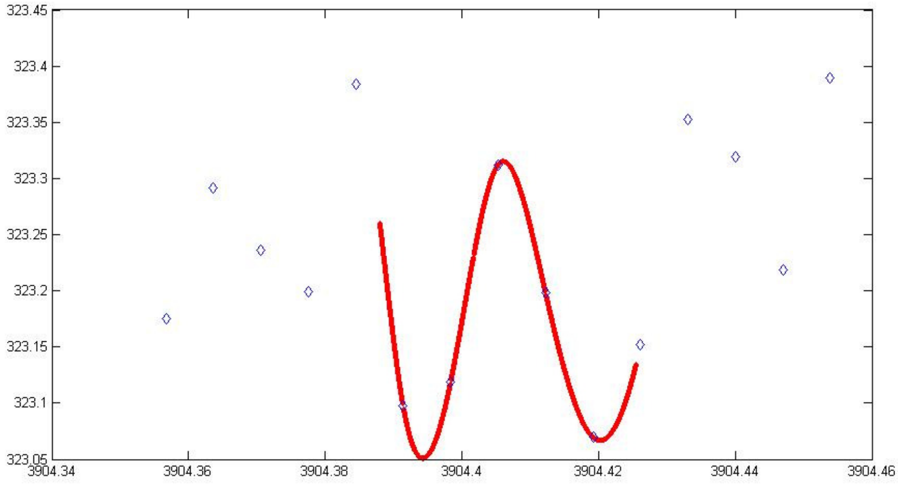

Figure 5: FWF Phase interpolation spline unaffected by an unlock in L1PP v3.5

2.4. RFI Mitigation Algorithms

2.4.1. Results Analysis

Figure 6 shows the impact of the mitigation algorithm in L1PP v3.4 and v3.5 for a snapshot over the Dominican Republic acquired on 08-Jul-2010 around 11:44.Note that there is no way on assessing on the quality of the mitigation since there is no actual truth to compare the different results.

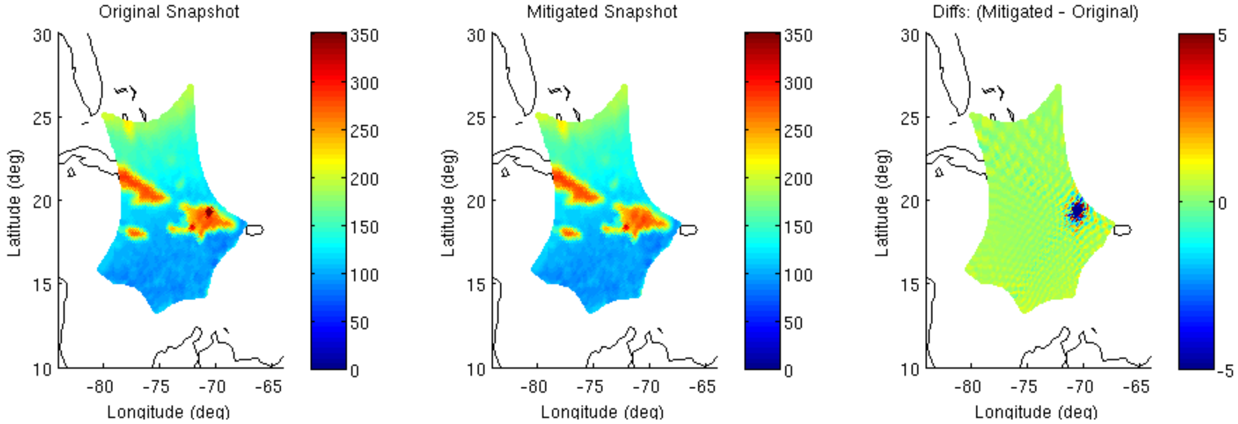

Figure 6: Mitigation algorithms in L1PP - Snapshot ID 35740255 (V-pol)

The only method to assess on the effectiveness of the mitigation algorithm is to compute the difference between two snapshots – the original one and the mitigated one. By visual inspection, the RFI seems to have been correctly removed since the difference plot concentrates the biggest part of the difference in the region where the RFI was located, and no significant changes are observed in the rest of the Alias Free Field of View and Extended region.

2.5. RFI Flagging Algorithms

2.5.1. Results Analysis

The RFI flagging mechanisms are triggered at L1b and L1c. For L1b the flags are set at a snapshot level and there are only two values: snapshot is/isn't corrupt by RFI and RFIs have/haven't been mitigated on current snapshot. For the L1c, there are three possible flagging mechanisms: to flag the pixels contained in a circle around the RFI position, to flag the pixels covered by the tails formed by the RFI or to flag all the pixels in the snapshot as corrupt. The circle radius is computed for each RFI and is dependent on its BT, as listed in the AUX_RFILST, and is used to compute the width of the tails formed by the RFI.

In Figure 7 two examples are presented illustrating the flagging of circle and tails for different RFIs in distinct zones of the snapshot.

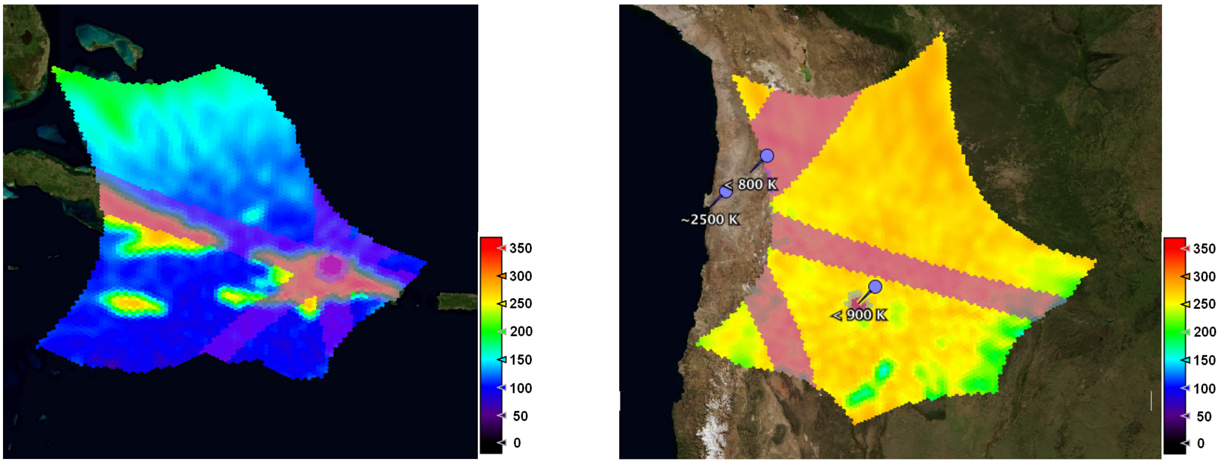

(a) $T_{B,RFI}$ = 1230 K, V-pol *(b) $T_{B,RFI}$ indicated in the pins, V-pol*

Figure 7: Flagging algorithms in L1PP. BT values used to compute the radius

These algorithms have no impact related to the structure of the products. All flags described in the section above have been implemented using already existing bits in the flags field, as described in [RD.6].